Impact of the Cellular Prion Protein on Amyloid-β and 3PO-Tau Processing

Matthias Schmitz[a,*], Katharina Wulf[a], Sandra C. Signore[b], Walter J. Schulz-Schaeffer[c],
Pawel Kermer[b], Mathias Bähr[b], Fred S. Wouters[d], Saima Zafar[a] and Inga Zerr[a]
[a]*Department of Neurology, Clinical Dementia Center and University Medical Center Göttingen,
Göttingen, Germany*
[b]*Department of Neurology, University Medical Center Göttingen, Göttingen, Germany*
[c]*Department of Neuropathology, University Medical Center Göttingen, Göttingen, Germany*
[d]*Laboratory for Molecular and Cellular Systems at the Institute for Neuro- & Sensory Physiology,
Göttingen, Germany*

Abstract. Previous studies indicate an important role for the cellular prion protein (PrP^C) in the development of Alzheimer's disease (AD) pathology. In the present study, we analyzed the involvement of PrP^C in different pathological mechanisms underlying AD: the processing of the amyloid-β protein precursor (AβPP) and its interaction with AβPP, tau, and different phosphorylated forms of the tau protein (p-tau). The effect of PrP^C on tau expression was investigated in various cellular compartments using a HEK293 cell model expressing a tau mutant (3PO-tau) or wild type (WT)-tau.

We could show that PrP^C reduces AβPP cleavage, leading to decreased levels of Aβ$_{40}$ and sAβPP without changing the protein expression of AβPP, β-secretase, or γ-secretase. Tau and its phosphorylated forms were identified as interactions partners for PrP^C, raising the question as to whether PrP^C might also be involved in tau pathology. Overexpression of PrP^C in *PRNP* and 3PO-tau transfected cells resulted in a reduction of 3PO-tau and p-tau as well as a decrease of 3PO-tau-related toxicity. In addition, we used the transgenic PrP^C knockout (*Prnp0/0*) mouse line to study the dynamics of tau phosphorylation, an important pathological hallmark in the pathogenesis of AD *in vivo*. There, an effect of PrP^C on tau expression could be observed under oxidative stress conditions but not during aging. In summary, we provide further evidence for interactions of PrP^C with proteins that are known to be the key players in AD pathogenesis. We identified tau and its phosphorylated forms as potential PrP-interactors and report a novel protective function of PrP^C in AD-like tau pathology.

Keywords: Alzheimer's disease, amyloid, β-secretase, cellular prion protein, neuroprotection, 3PO-tau, p-tau

INTRODUCTION

The cellular prion protein (PrP^C) is a highly conserved glycosylphosphatidylinositol (GPI)-anchored protein with a variety of functions such as copper binding, regulation of the circadian rhythm, and protection against oxidative stress [1–3].

Similar to tau and amyloid-β protein precursor (AβPP), PrP^C is localized in lipid rafts [4], which are strongly involved in signal transduction, e.g., through src kinases (Fyn/Erk1/2 activation) or receptor tyrosine kinases [5–7]. Previous studies indicated an association of PrP^C with the cytoskeleton, where it modulates the expression of certain cytoskeletal proteins [8], and it may interact with tubulin [9–11]. Binding of PrP^C to tubulin results in tubulin oligomerization and inhibition of microtubule formation [12]. Therefore, we now studied in detail its interaction with the tau protein, which is an important component of the microtubule cytoskeleton.

Besides its protective function under ischemic stress conditions [3, 13–15], evidence is accumulating that PrP^C may play a role in Alzheimer's disease (AD)

---
*Correspondence to: Matthias Schmitz, Department of Neurology, Clinical Dementia Center and University Medical Center Göttingen, Göttingen, Germany. Tel.: +49 5513910454; E-mail: matthias.schmitz@med.uni-goettingen.de.

or during the development of AD-like pathology: 1) On a neuropathological level, PrP^C co-localizes with amyloid plaques [16, 17] which are present in Creutzfeldt–Jakob disease (CJD) patients with amyloid pathology [18]; 2) In humans, codon 129 polymorphism of the human PrP^C gene, resulting in either methionine or valine, influences the susceptibility to prion diseases. Furthermore, certain amino acid variations may also be a risk factor for early onset AD [19, 20] and the codon 129 polymorphism can modulate the number of amyloid deposits during cerebral aging [21]; 3) In disease models, the role of PrP^C in the development of AD-like pathology remains puzzling. Clear evidence exists that PrP^C is involved in the pathophysiological metabolism of AβPP. PrP^C contains an amyloid oligomer binding site, a region within the central part of PrP^C from amino acid 95–110 [22]. PrP^C thus may act as a potential receptor for amyloid-β (Aβ) mediating the toxicity of Aβ oligomers as shown in an AD mouse model [23, 24]. Aβ oligomers are thought to induce neuronal deficits in synaptic plasticity or neuronal cell death and the animals can be rescued when PrP^C is knocked out [22] or by treatment with antibodies directed against PrP^C [25]. Moreover, they can modulate the trafficking and expression of PrP^C on the cell surface, a fact which lends further support to the hypothesis of a mutual interference between Aβ and PrP^C [26].

Nevertheless, three independent studies failed to confirm the postulated PrP^C-promoted toxic effects [27–29] leaving the debate on the role of PrP^C still open.

In addition to amyloid plaques, the second major hallmark in AD is the formation of neurofibrillary tangles, consisting of hyperphosphorylated tau protein. Phosphorylation of tau protein at different sites is central to its pathologic effect, and its regulation occurs independently by different kinases. Therefore, we focused on different phosphorylated tau isoforms which are related to AD pathology. An interaction of PrP^C and tau protein has already been demonstrated [30], suggesting a novel function of PrP^C in the metabolism of tau under physiological and/or AD conditions. Whether this interaction results in a change in tau expression or phosphorylation remains unclear.

In the present study, we investigated the interaction of PrP^C with AβPP, tau, p-tau Thr-181, and p-tau Ser-396 and the impact of PrP^C on the processing of AβPP. The effect of PrP^C on tau-induced toxicity was analyzed in a human embryonic kidney 293 (HEK293) cell model co-expressing PrP^C and a mutant form of tau (3PO-tau) that exhibits high toxicity, aggregation,

and phosphorylation [31]. In *Prnp0/0* mice, we investigated the effects of aging and oxidative stress on the expression of tau and several isoforms of p-tau in comparison to wild type (WT) mice.

MATERIALS AND METHODS

Cell culture

All chemicals were of analytical grade and obtained either from Sigma-Aldrich (Taufkirchen, Germany) or Merck (Darmstadt, Germany). HEK293 cells and SH-SY5Y, human neuroblastoma cells, were grown in Dulbecco's modified Eagle medium (DMEM, Sigma-Aldrich), supplemented with 10% fetal calf serum (Biochrom, Berlin, Germany), 1% penicillin/streptomycin, and 1% L-glutamine (only for SH-SY5Y) (Biochrom) under standard culture conditions (37°C, 5% CO$_2$ supply, and 95% humidity). Both cell lines were split 1–2 times per week and the medium was exchanged at least every four days. The 293 cell line was derived by transformation of primary cultures of HEK cells with sheared adenovirus (Ad) 5 DNA. They behave similarly to neuronal cells [32].

Cell survival

Cell survival was assessed by crystal violet staining. Cells were fixed with 1% glutaraldehyde, washed with phosphate-buffered saline (PBS), and stained with crystal violet (0.02% in water). The amount of crystal violet bound to the cells was dissolved with 70% ethanol. Data collection was performed with a spectrophotometer at a wavelength of 550 nm.

Transfection

HEK293 and SH-SY5Y cells were transiently transfected with the pCMS-*PRNP*-EGFP vector, expressing human PrP^C gene (*PRNP*). An empty pCMS-EGFP vector was used as control. The generation of WT- and 3PO-tau-GFP vectors was described in detail by Iliev et al. [31]. Plasmids were purified using the EndoFree Maxi Kit (Qiagen GmbH, Hilden, Germany). For the transfection, $1–1.5 \times 10^6$ cells were seeded in a six well plate for 24 h. 1.5–2 μg of plasmid DNA and 4–6 μl lipofectamine (Invitrogen, Groningen, Netherlands) were dissolved in 250 μl OptiMEM (Gibco/Invitrogen, Karlsruhe, Germany) for 5 min. Stable DNA complexes were formed after 20–30 min and pipetted to the transfection medium (OptiMEM containing 2% FCS), in which the cells were incubated

for 6–8 h or overnight. Thereafter, the transfection medium was replaced by fresh culture medium. After 48 h, cells were washed in PBS and scraped on ice in cell-lysis buffer consisting of 50 mM Tris-HCL pH 8.0, 150 mM NaCl, 1% Triton X-100, and a protease- and phosphatase inhibitor cocktail (Roche, Mannheim, Germany).

Transfected cells could be distinguished from non-transfected cells by the EGFP fluorescence (Supplementary Fig. 1). We quantified the transfections efficiencies. While *PRNP* has a transfections efficiency of approximately 80%, we observed an efficiency of 70% for 3PO tau. Consequently, we obtained more than 50% of double transfectants.

Animals

For each experiment, at least five adult male *Prnp* knockout mice (designated *Prnp0/0*) and WT mice aged between 3 and 15 months were used. The genetic background of both *Prnp0/0* and WT mice was derived from both 129/Sv and C57BL/6 [33]. *Prnp0/0* mice are homozygous for the disrupted PrP^C gene (*Zurich I*), produced as previously described by Bueler et al. [33]. The transgenic mouse line 35 (Tg35) carries a cosmid transgene encoding the mouse PrP b allele which leads to an 8–10 times overexpression of mouse PrP^C in the brain.

Mice were housed, under controlled temperature conditions (21–22°C), with free access to food and water in a 12 : 12 h light:dark cycle. The body weight of all animals varied between 25 and 35 g. All protocols used were in accordance with the ethical rules for animal experiments.

After mice were euthanized, brains were collected either whole or were dissociated on ice into three brain regions (hippocampus, cortex, and cerebellum). Subsequently, whole brains/brain regions were separated, complemented with lysis buffer containing 50 mM Tris HCl (pH 7.5), 150 mM NaCl, 2 mM EDTA, 1% Triton X-100, and protease/phosphatase inhibitor cocktail and homogenized. Brain lysate samples were incubated in a tube rotator (Schuett Labortechnik GmbH, Goettingen, Germany) for 15 min and centrifuged at 4°C at 13000× *g*. Supernatants were transferred into separate tubes and stored at −80°C.

Induction of transient focal cerebral ischemia

Animals were anaesthetized with 1%–1.5% isoflurane (30% O$_2$, 70% N$_2$O). Rectal temperature was maintained at 36.5–37°C using a feedback-controlled heating system. In order to assess cerebral blood flow, laser-Doppler flow was recorded during all experiments using a 0.5 mm fiberoptic probe (Perimed, Sweden) attached to the skull overlying the core region of the middle cerebral artery (MCA) territory (2 mm posterior, 6 mm lateral from bregma). Focal cerebral ischemia was induced by transient occlusion (60 min) of the MCA using the intraluminal filament technique. Following a midline neck incision, the left common and external carotid artery were isolated and ligated. After placing a microvascular clip (Aesculap, Germany) on the internal carotid artery, an 8-0 silicon resin (Xantopren, Deuker, Germany) coated nylon monofilament (Ethilon; diameter 180 to 200 μm; Ethicon, Germany) was introduced through an incision into the distal part of the common carotid artery and, after clip removal, advanced 9 mm distal from the carotid bifurcation for MCA occlusion. The monofilament was withdrawn after 60 min of ischemia to allow reperfusion of the MCA. Laser-Doppler flow recording continued for 15 min to monitor appropriate reperfusion.

Immunohistochemical staining

Cells or brain tissue were fixed in PBS containing 4% formaldehyde for 20 min, washed 3 times with PBS and permeabilized by incubation in PBS containing 0.2% Triton X-100 for 10 min. Permeabilization was followed by 1 h blocking in PBS containing 2% bovine serum albumin (BSA). Subsequently, the specimens were incubated with primary antibody diluted 1 : 500 in PBS containing 1% BSA for 2 h at room temperature. All steps were carried out in a dark humidified chamber and were stopped by washing three times with PBS. Finally, stained material was mounted in Mowiol 4–88 (Roth, Karlsruhe, Germany) before examination of the staining under an Olympus BX51 microscope (Olympus, Hamburg, Germany) could be performed. Images were acquired and processed using cell F-software (Olympus).

Immunoprecipitation analysis

HEK293 cells were scraped on ice in PBS containing a cocktail of protease and phosphatase inhibitors and were sonicated. Afterwards, insoluble cell debris was removed by centrifugation at 5400× *g* for 15 min at 4°C. Protein G or A dynabeads (Invitrogen) were used for the immunoprecipitation according to the manufacturer's instructions. Briefly, 4 μl antibody and 315 μg protein were incubated in a tube rotator (Schuett

Labortechnik) for 1 h at 4°C. Afterwards, 50 μl of 50% slurry Dynabeads were added into each vial and incubated with rotation overnight at 4°C, followed by three washing steps before the target antigen could be eluted. Immunoprecipitated proteins (2×10^6 cells/protein) were investigated by SDS-PAGE and western blotting.

Enzymatic deglycosylation of PrP^C

PrP^C-containing samples were deglycosylated using a glycoprotein deglycosylation kit (Calbiochem/Merck, Darmstadt, Germany). The procedure was carried out according to the manufacturer's instructions. After addition of reaction and denaturation buffer, samples were heated for 5 min at 95°C. After cooling to room temperature, N-glycosidase F was added. Thereafter, the samples were incubated for 3 h at 37°C.

Protein extracts preparation and subcellular fractionation

Cells were washed, scraped in ice-cold PBS, and pelleted. Lysates were prepared using a buffer containing 50 mM Tris-HCl, pH 7.4, 150 mM NaCl, 1% Triton X-100, and complete protease inhibitor cocktail (Roche, Indianapolis, IN, USA) for 15 min at 4 C, followed by 10 min centrifugation at 16,000 g at 4 C. The pellets, which were further used for the filter retardation assay, were resuspended in lysis buffer and sonicated. Subcellular fractionation was performed using a ProteoExtract Subcellular Proteome Extraction Kit (Calbiochem, San Diego, CA, USA) according to the manufacturer's instructions. Unless stated otherwise, cells were analyzed 24 h post-transfection. The immunoblotting was done with the following antibodies: AT8 AK (Thermoscientific, Bonn, dilution 1 : 1000), anti-tau T46 (Invitrogen, dilution 1 : 1000), mouse anti-histone 2B (Abcam, Milton, GB, dilution 1 : 2000), mouse anti-beta actin (Abcam, dilution 1 : 5000), and mouse anti-cadherin (Sigma-Aldrich, St. Louis, USA, dilution 1 : 2000).

SDS-PAGE and immunoblotting

For western blot analysis, we used the monoclonal PrP antibodies SAF32 and 12F10 (SPI-Bio, Paris, France) diluted at 1 : 500; monoclonal anti-AβPP (Millipore, Schwalbach, Germany), polyclonal anti-BACE1, and polyclonal anti-p-tau Ser-396 (Acris Antibodies, Herford Germany) diluted at 1 : 1000; polyclonal anti-tau and polyclonal anti-p-tau

Thr-181 (Abcam, Cambridge, UK) diluted at 1 : 1000; monoclonal anti-p-tau Ser-199 (Roboscreen, Leipzig, Germany) diluted at 1 : 500; and monoclonal mouse anti-β-actin (Abcam) diluted at 1 : 15000. After adding loading buffer (Bio-Rad, Munich, Bavaria, Germany), samples were heated for 2 min at 95°C.

Samples were separated by sodium dodecyl sulfate-polyacrylamide gel electrophoresis (SDS-PAGE) (12% w/v polyacrylamide) and transferred to polyvinylidene difluoride (PVDF) Hydrobond-P membranes (Amersham, Freiburg, Germany) using a semi-dry transblot cell (Bio-Rad) for 60 min at 12 Volt. Afterwards, PVDF-membranes were blocked with 5% dried skimmed-milk powder in PBS and 0.1% Tween-20 (PBST) for 1 h at room temperature and probed with the primary antibody overnight at 4°C. Membranes were washed in PBST and incubated with the corresponding horseradish peroxides conjugated secondary antibody (Jackson Immuno Research, Leipzig, Germany) diluted at 1 : 10000 for 1 h. Protein bands were visualized after immersion of the membranes in enhanced chemiluminescence (ECL) detection solution and analyzed using the Chemi-Doc (Bio-Rad). All western blots shown are representative of at least three different and independent experiments.

Analysis of Aβ$_{40}$, sAβPPβ, and sAβPPα concentration by enzyme linked immunosorbent assay (ELISA)

Levels of Aβ$_{40}$ were ascertained using the amyloid beta (1-40) (N)-assay and the highly specific mouse amyloid beta (1-40) ELISA obtained from (IBL, Hamburg, Germany). The amyloid beta (1-40) (N) assay kit is designed to measure full-length amyloid beta (1-40) peptides with an intact N terminus. It uses the anti-amyloid beta (35–40) (1A10) antibody as the capture antibody and an HRP-conjugated anti-human Aβ-(N) rabbit IgG polyclonal antibody as a detection antibody. Levels of sAβPPβ were determined by the use of the anti-human sAβPPβ kit employing 6A1 mouse IgG and sAβPPα was analyzed by the anti-human sAβPPα kit with the monoclonal mouse IgG 2B3 (IBL, Hamburg, Germany).

All ELISA measurements were performed according to the protocol of the manufacturer. Samples with an adapted protein concentration of either 20 or 40 μg total protein were sonicated and diluted in EIA buffer to a volume of 100 μl. The colorimetric reaction was measured at 450 nm with a 1420 Multilabel Counter Victor 2 (Wallac) (PerkinElmer, Massachusetts, USA).

Analysis of tau and p-tau concentration

We used a tau and p-tau threonine Thr-231 multiplex assay as developed by Meso Scale Discovery™ (MSD) (Rockville, USA) and followed the manufacturer's instructions. The MSD ECL platform requires the use of special plates with embedded carbon ink electrodes. The principle of electrochemiluminescence is based upon electrochemical stimulation of an antibody SULFO-TAG label [ruthenium(II) tris-bipyridine-(4-methylsulfonate) NHS ester] label. This leads to the emission of light at 620 nm which could be detected by a CCD camera in the MSD Sector Imagers.

After blocking with BSA for 1 h, pre-coated plates were incubated with 40 μg brain homogenate for 1 h. After washing, the signal is detected using sulfo-tag labeled detection antibodies against tau and p-tau. The plates were analyzed using the MSD Sector Imager.

Determination of the γ-secretase concentration

We used a commercial Human γ-Secretase ELISA Kit (Cusabio, Wuhan, China) to analyze brain homogenates derived from *Prnp0/0* and WT mice. The kit is based on ELISA techniques and is eligible for the qualitative determination of human γ-secretase. Brain homogenate samples were adapted to a total protein amount of 2 μg and measured according to the manufacturer's instruction.

Determination of the PrP concentration

Sonicated cell samples were analyzed by a commercial BetaPrion BSE-ELISA Test Kit (AJ Roboscreen, Leipzig, Germany). The kit is based on ELISA techniques and is eligible for a rapid BSE test for the qualitative determination of PrP^{res} in the brain of cattle and sheep. We omitted the proteinase (PK) digestion step. Our aim was to measure the concentration of total PrP^C. Cell samples were adapted to a total protein amount of 5 μg and measured according to the manufacturer's instruction.

Statistical analysis

The quantification of the band intensities was performed by using the *Scion Image* software. All data were evaluated by the statistic software *Graph Pad Prism 4*. We calculated the *p* values by using the *student's t-test* for values which are normally distributed. Non-normally distributed values were analyzed by the Wilcoxon-Mann-Whitney-Test (Mann-Whitney-U-Test). The standard errors of the mean (SEM) were depicted as error bars. All values with $p < 0.05$ were considered significant.

RESULTS

Interaction of PrP^C with AD relevant proteins in HEK293 cells

The interaction of PrP^C with AD-relevant proteins (AβPP, tau, p-tau) was investigated in *PRNP*-transfected HEK293 cells.

Immunoprecipitation of PrP^C using monoclonal PrP^C antibody (SAF32) followed by western blotting with antibodies against AβPP, tau, p-tau Thr-181 and p-tau Ser-396 revealed a protein band of the expected molecular weight of the respective protein (Fig. 1). In addition, we examined the immunoprecipitates of AβPP, tau, p-tau Thr-181, and Ser-396 for PrP^C. Their co-immunoprecipitation was indicative of a direct or an indirect interaction of PrP^C with these proteins (Fig. 1).

For the detection of AβPP, we used the mAb 22C11, which recognizes full-length and a secreted isoform of AβPP (sAβPP) (MW 100 kDa) [34, 35]. It is worth noting that we detected a faint band with the size of approximately 130 kDa corresponding to full-length AβPP and a more intensive band corresponding to sAβPP (MW 100 kDa) in the PrP^C immunoprecipitate (Fig. 1A). These data indicated that sAβPP possesses a higher affinity to PrP^C than full-length AβPP.

No interaction was evident when the Dynabeads were incubated with non-specific mouse or rabbit IgG. For each protein, total protein extracts (Input) showed the same molecular weight of the analyzed proteins (Fig. 1).

Impact of PrP^C on the expression of AβPP, BACE1, and on AβPP cleavage fragments

HEK293 cells were transiently transfected with the pCMS-*PRNP*-EGFP vector, expressing human *PRNP* and an empty pCMS-EGFP vector [31]. Western blot analysis of cell lysates using the monoclonal antibody SAF32 demonstrated the expression of PrP^C 24 h and 48 h after transfection as compared to control cells that exhibit the endogenous level of PrP^C (Fig. 2A1). We observed a molecular weight of 27 kDa for the unglycosylated, 33 kDa for the monoglycosylated, and 35 kDa for the diglycosylated PrP^C isoform. Treatment with N-glycosydase F (PNGase F) was used to deglycosylate PrP^C and to prove the specificity of the PrP^C detection (Fig. 2A2). A densitometric evaluation of the band intensities as well as the determination of the
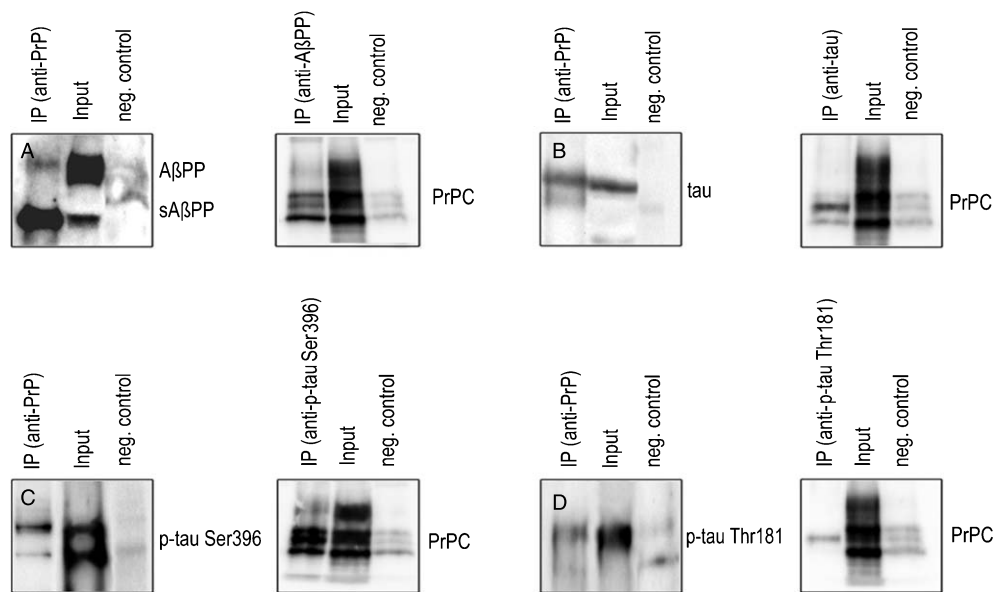
Fig. 1. Interaction of PrP^C with sAβPP, AβPP, tau, and p-tau. Lysates from PrP^C overexpressing HEK293 cells were immunoprecipitated (IP) first with anti-PrP SAF32 and secondly with the indicated antibodies. As potential interacting partners of PrP^C, the proteins AβPP and sAβPP (A), tau (B), p-tau Ser-396 (C), and p-tau Thr-181 (D) could be identified by western blotting. Total protein extract from cell lysates (Input) was loaded as a positive internal control of electrophoretic mobility and antibody specificity. The negative control, consisting of beads without antibody, was shown for each antibody. All IPs were triplicates.

PrP^C concentration revealed a significant upregulation of PrP^C level between 3.5–4 fold 48 h after transfection (Figs. 2A1 and 3).

Moreover, we examined the expression of AβPP and BACE1 using immunoblotting in the same samples and showed that PrP^C had no impact on the expression of both proteins (Fig. 2B). The intra- and extracellular (conditioned cell media) levels of the AβPP cleavage fragments Aβ$_{40}$ and sAβPPβ, indicators for the amyloidogenic processing pathway, and sAβPPα, an indicator for the non amyloidogenic processing pathway of AβPP, were determined by ELISA (Fig. 2C). Overexpression of PrP^C resulted in a significant decrease of Aβ$_{40}$, sAβPPβ, and sAβPPα of approximately 20–30% as compared to control cells (Fig. 2C1-3). We confirmed these findings in the neuroblastoma cell line SH-SY5Y (Supplementary Fig. 1A-D).

In vivo studies were carried out on brain samples derived from *Prnp0/0* mice and WT mice at an age of 3 and 15 months. The quantification of protein bands in the western blot confirmed our observation that the presence or absence of PrP^C did not influence AβPP or BACE levels and this effect does not depend on age (Fig. 2D). When we analyzed the level of Aβ$_{40}$ by ELISA, it could be observed that *Prnp0/0* mice (at 3 and 15 months of age) contained a significant higher amount of Aβ$_{40}$ (40–50%) than WT animals of the same age (Fig. 2E1). Independently of PrP^C, no significant differences could be observed between young and old animals (Fig. 2E1).

As a further control, we used PrP^C overexpressing Tg35 mice, which showed a significant decreased level of Aβ$_{40}$ compared to WT and *Prnp0/0* mice (Fig. 2E2). The concentration of γ-secretase was measured in WT and *Prnp0/0* mice (3 months) by ELISA and revealed no significant abnormalities in *Prnp0/0* mice (Fig. 2E3). Since we used a non-AD-model, the amount of Aβ$_{42}$ was below the detection limit of the ELISA and therefore excluded from our study.

PrP^C reduces levels of 3PO-tau and p-tau and increases cell survival

3PO-tau is a mutant form of the full length tau protein. In this mutant, three single amino acid changes were made in the microtubule binding repeats that break predicted β-sheet-forming patterns of alternating polar and apolar amino acids, i.e., the mutant was three times pattern-optimized (3PO) for aggregation. These regions were later confirmed to contain β-sheet structure by solid-state NMR [36]. 3PO was shown in different cell types to form stable tau aggregates with highly phosphorylated tau protein, disruption of the
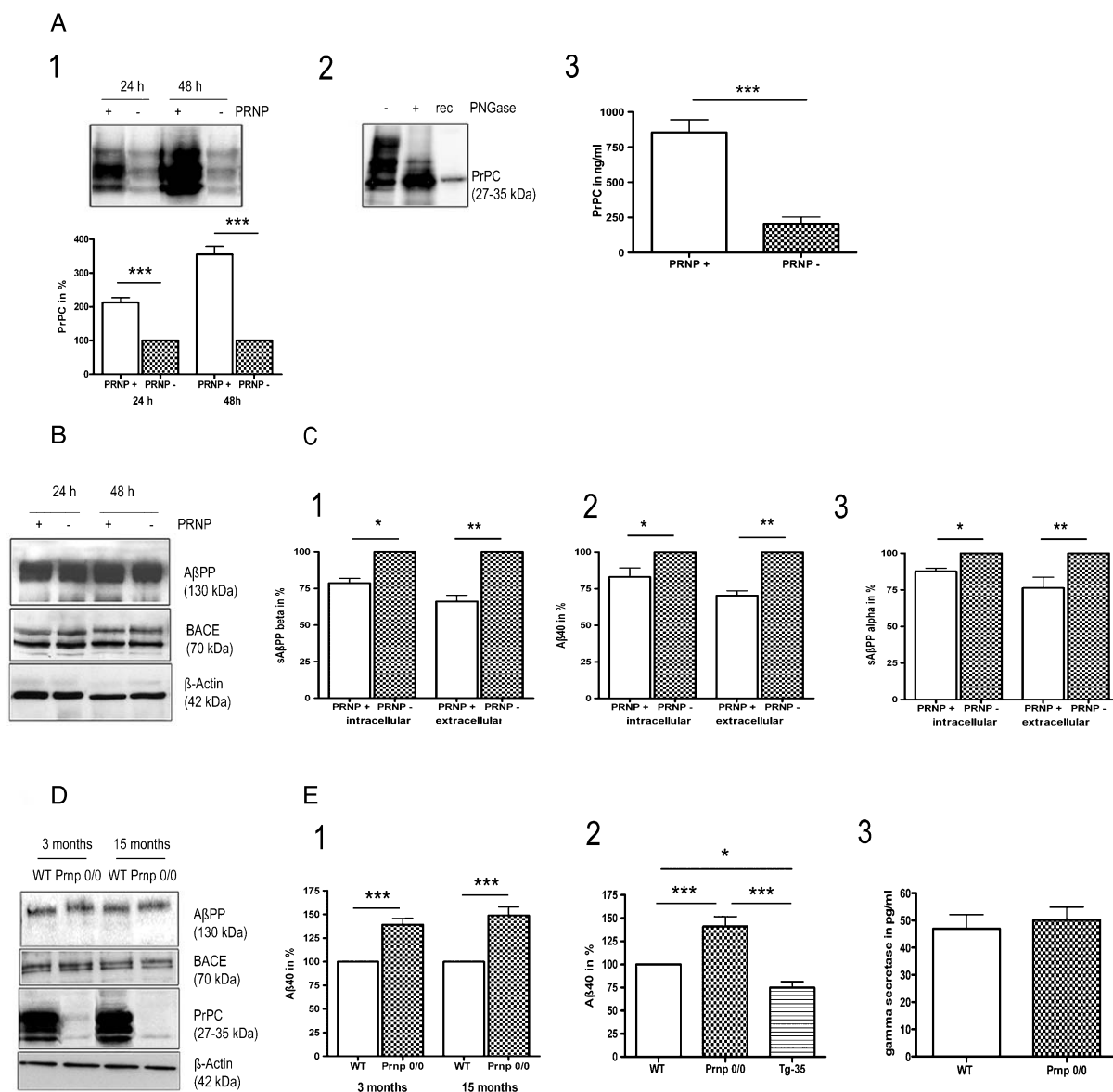
Fig. 2. Effect of PrP^C on the expression of AβPP, BACE1, Aβ$_{40}$, sAβPPβ, and sAβPPα. A) PrP^C overexpressing HEK293 cells were analyzed 24 and 48 h after transfection by western blotting in comparison to control cells (1). Quantification of the band-intensity showed that PrP^C was approximately 2-fold upregulated 24 h- and approximately 3.5 fold upregulated 48 h after transfection (1). Treatment with PNGase resulted in a deglycosylation of PrP^C to prove the specificity of the PrP^C detection (2). Concentration of PrP^C was determined 48 h after transfection using a PrP ELISA-assay (3). B) Expression of AβPP and BACE1 was analyzed 24 and 48 h after transfection by western blotting. Both proteins were not influenced by the expression of PrP^C. C) Amount of AβPP-cleavage fragments were measured via ELISA. Intra- and extracellular levels of Aβ$_{40}$, sAβPPβ, and sAβPPα were decreased significantly in PrP^C over-expressing cells (1–3). All *in vitro* experiments were carried out at least in triplicates. D) In mice, analysis of AβPP and BACE1 expression revealed no differences between *Prnp0/0* and WT mice. E) ELISA measurement of Aβ$_{40}$ generation in mice brains revealed a marked, age-independent increase in *Prnp0/0* mice compared to WT animals (1). PrP^C overexpressing Tg35 mice revealed a decreased level of Aβ$_{40}$ (2) whereas concentration of γ-secretase remained unchanged in *Prnp0/0* mice (3). All values were calculated in % of WT. Beta actin was used as an internal standard. For comparison between groups we used the *student's t-test* ($n = 5$ per group in three independent experiments). Error bars indicate standard errors of the mean (SEM).

microtubule network, and strong cell death [31]. 3PO-tau expression in rodent brain using viral delivery also produced a strong AD-like pathology [37].

In the present study, we transiently co-transfected HEK293 cells with 3PO-tau and *PRNP*. Control cells were transfected with 3PO-tau and an empty vector

(lacking the *PRNP* gene). To investigate the cellular distribution of 3PO-tau, we performed a subcellular fractionation into cytosolic, membranous/organellar, nuclear, and cytoskeletal fractions. Afterwards, expression of 3PO-tau (Fig. 3A) and p-tau (Fig. 3B) were analyzed by western blotting. In addition to a band running at 75 kDa, which probably corresponds to monomeric full length 3PO-tau, we could detect several protein bands between 20 and 30 kDa, which we consider to be proteolytical tau fragments. In 3PO-tau transfected cells, we observed additional bands at 20–25 kDa, which likely indicated an increased fragmentation of 3PO-tau (Fig. 3A). The expression of these tau forms was depicted 60 h after transfection. Band intensities of the immunoblots were quantified using densitometric analysis. Interestingly, 3PO-tau and p-tau were found equally abundant in the cytosolic and cytoskeletal fractions, which are of particular interest, because the main toxicity of tau in AD is related to the destruction of the microtubule system. They were less abundantly detectable in the membrane/organelle fractions (Fig. 3A, B).

Our data revealed that overexpression of PrP^C resulted in a significant decrease of 3PO-tau and its phosphorylated forms (p-tau) in all subcellular compartments (Fig. 3A, B), indicating a protective role of PrP^C in tau metabolism and tau induced AD-like pathology. Even though PrP^C is a ubiquitously expressed protein, the amount of tau down regulation also depends on the cellular environment; in particular the cytoskeleton-associated 3PO-tau and p-tau levels were decreased when cells were co-transfected with PrP^C (Fig. 3A, B). Aggregated 3PO-tau can be observed in the cytoskeletal fraction as a band over the prominent 70 kDa monomeric protein band (Fig. 3A). Expression of PrP^C completely eliminates this higher fraction, suggesting that tau aggregation is reduced.

In accordance with the lower overall 3PO-tau levels, its phosphorylation and aggregation, toxicity in 3PO-tau-*PRNP*-co-transfected cells was significantly lower than in control cells co-transfected with 3PO-tau and an empty vector. This could be shown in a crystal violet cell survival assay. Here, a co-transfection with *PRNP* resulted in a significantly increase of the survival rate of these cells (Fig. 3C).

Additionally, we also found that overexpression of PrP^C resulted in a significant decrease of WT-tau in all subcellular compartments (Supplementary Fig. 3). This seems to indicate that PrP^C exerts its neuroprotective effect by mechanisms that act on both non-pathological and pathological tau. It should be noted that high expression levels of tau are neuro-

toxic [38] and this may indicate that PrP^C also plays a protective role in these forms of tauopathies.

Effect of PrP^C on tau and p-tau levels during aging and under oxidative stress conditions

We examined the effect of PrP^C on the expression of tau and p-tau in brain tissue derived from WT and *Prnp0/0* mice under both aging and oxidative stress conditions.

Expression of tau and p-tau Ser-199 in cortex, hippocampus, and cerebellum were illustrated by immunohistochemical staining. PrP^C had no significant effect on tau and p-tau localization as is depicted by the signal intensities and patterns observed in Fig. 4A.

The concentration of tau and p-tau Thr-231 in brain tissue of *Prnp0/0* and WT mice was determined by a MSD-electrochemiluminescence based assay. While aging (after 3 and 15 months) had no effect on tau and p-tau level neither in *Prnp0/0* nor in WT mice (Fig. 4B; Supplementary Fig. 2A), we observed an effect of PrP^C on the expression of tau under oxidative stress conditions (Fig. 4C). Six and 24 h after induction of a 60 min stroke, brain homogenates were analyzed by MSD-electrochemiluminescence based assay for tau and p-tau Thr-231. Interestingly, in *Prnp0/0* mice, the tau level increased after 6 and 24 h reperfusion as compared to normoxic *Prnp0/0* mice and WT mice under the same conditions (Fig. 4C). Levels of p-tau Thr-231 remained unchanged by PrP^C (Fig. 4C). An overview of the different p-tau isoforms is given in Supplementary Table 1.

DISCUSSION

Both AD and CJD are neurodegenerative diseases caused by conformational changes in specific proteins that alter their function. Co-existence of AD pathology in prion diseases such as CJD has already been shown [39] and a potential role of PrP^C in AD-like pathology is widely discussed [22–24].

However, the exact function of PrP^C on AD-relevant pathways has not yet been completely understood. The present study was undertaken to gain new insights into the physiological role of PrP^C and its interactions with proteins involved in the Aβ cascade hypothesis and in the development of tau pathology. In particular, we were interested in examining whether PrP^C may interact or regulate the expression of AD-relevant proteins namely AβPP, BACE1, Aβ, tau, or p-tau. We also analyzed the impact of PrP^C on the processing of
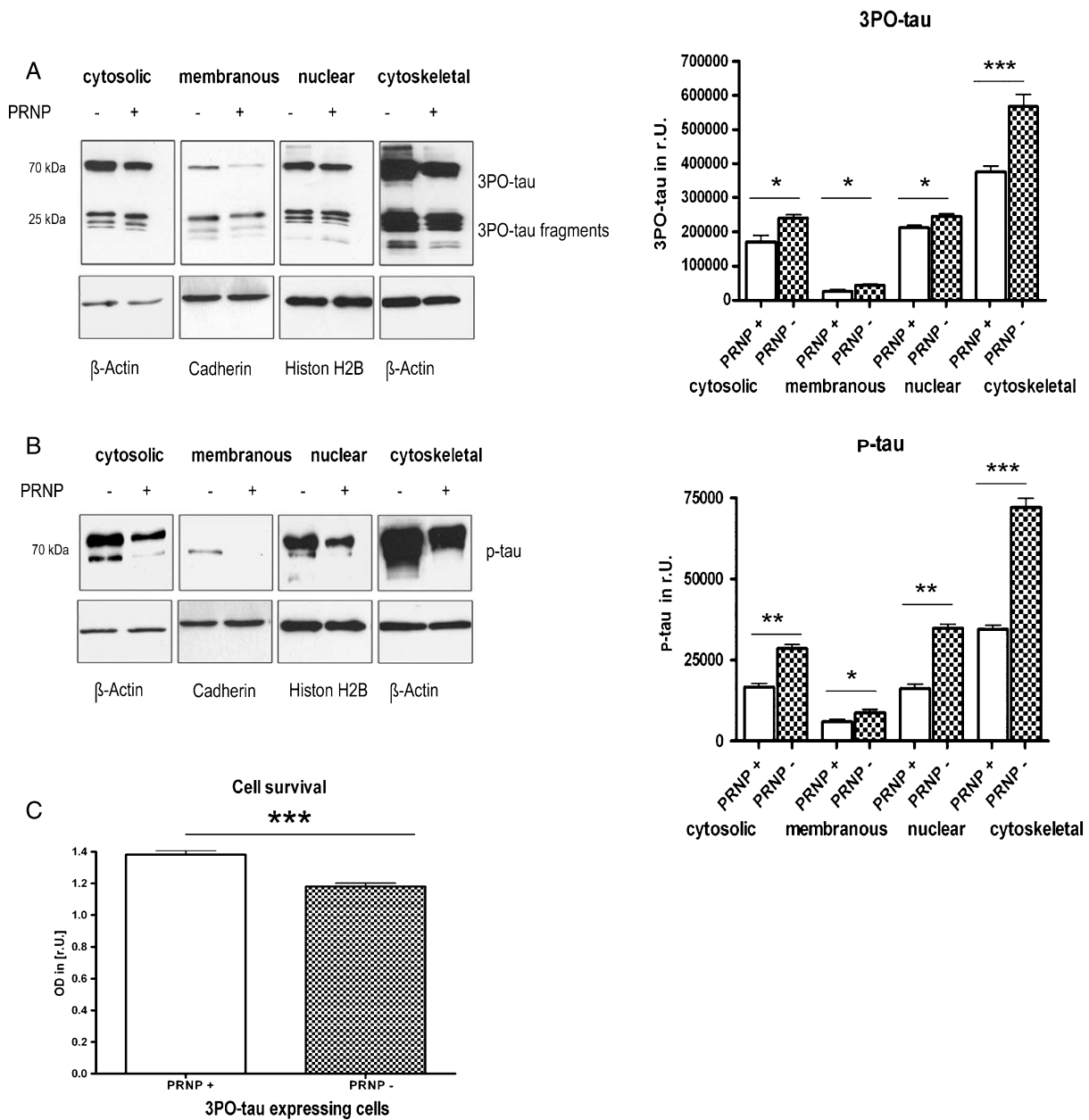
Fig. 3. Effect of PrP^C concentration on the expression of 3PO-tau and p-tau in different subcellular compartments. HEK293 cells were co-transfected with 3PO-tau and *PRNP* in comparison to control cells (3PO-tau and an empty control vector, designated as *PRNP-*), subjected to subcellular fractionation and immunoblotting. Four subcellular fractions (cytosolic, membranous/organelle, nuclear, and cytoskeletal) of co-transfected cells were analyzed 60 h after transfection by western blotting using the anti-C-terminal anti-tau T46 and anti-p-tau AT8. We used compartment-specific proteins as loading controls (bottom). A) Densitometric quantification of the band intensities revealed that 3PO-tau levels were significantly reduced in all subcellular compartments after 60 h, when PrP^C was overexpressed compared to control cells exhibiting an endogen PrP^C expression. B) Quantification of p-tau level (Thr-205 and Ser-202) of 3-PO tau co-transfected cells showed a decreased amount of p-tau in all cellular compartments when PrP^C is overexpressed compared to control cells exhibiting an endogen PrP^C expression. Densitometric analyses were performed from at least three different western blots. C) Co-transfected 3PO-tau cells (either with *PRNP* or with an empty vector) were cultivated for 60 h and analyzed in a crystal violet cell survival assay. Cellular survival was significantly increased in *PRNP+* cells in comparison to control cells (*PRNP-*). Cell survival was measured in triplicates, $n = 20$. For comparison between groups we used the *student's t-test*. Error bars indicate standard errors of the mean (SEM).
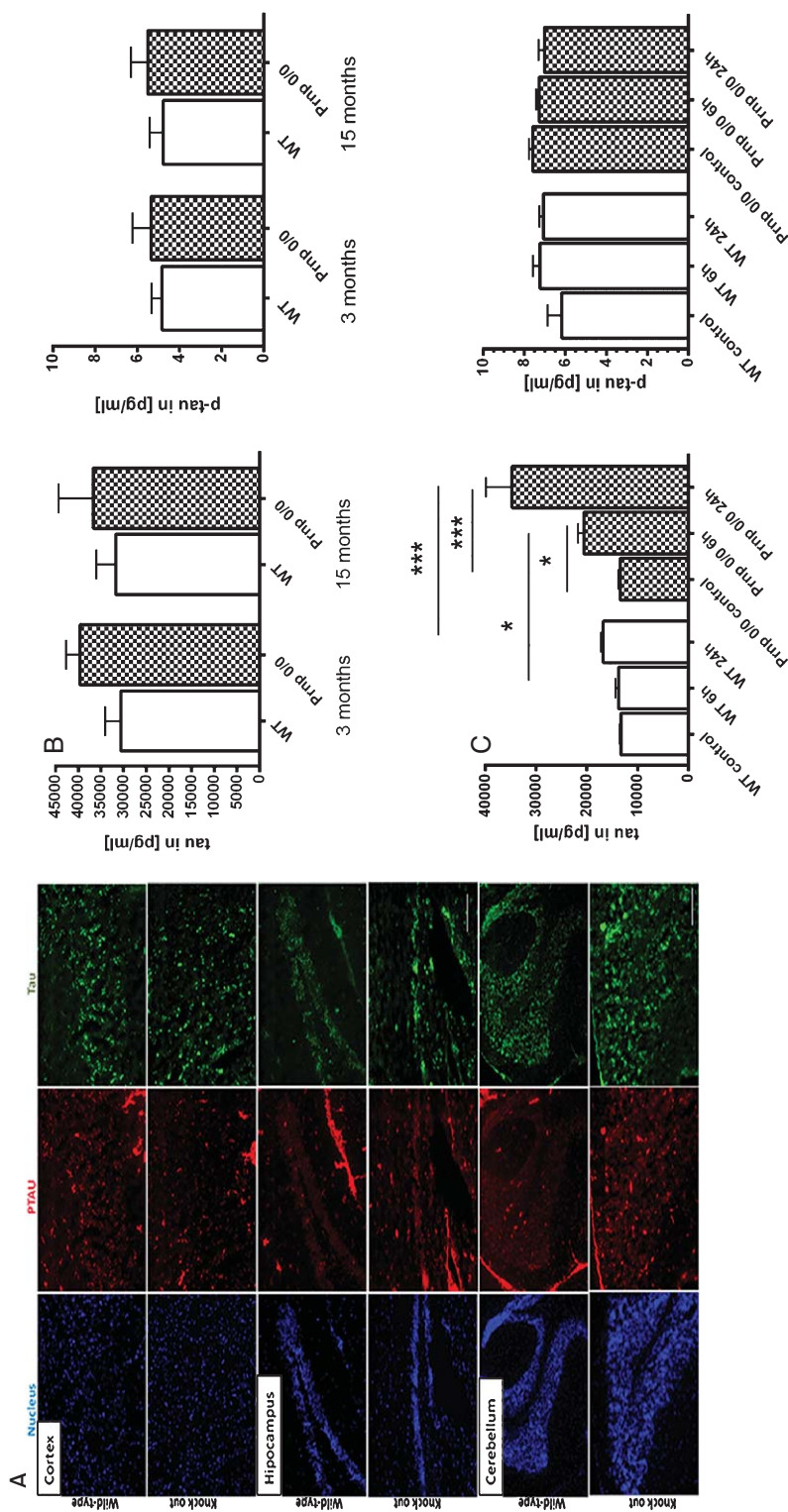
Fig. 4. PrP^C may influence expression of tau but not p-tau under ischemic-stress condition but not during aging. A) Expressions of tau and p-tau Ser-199 in different brain regions (cortex, hippocampus, cerebellum) were depicted via immunohistochemical staining. B, C) Amount of tau and p-tau Thr-231 were determined by MSD-electrochemiluminescence based assay in WT and *Prnp0/0* mice at different ages (B) and after experimentally induced transient focal cerebral ischemia (C). No major differences were found in *Prnp0/0* mice after 3 and 15 months of age. Six and 24 h after induction of ischemia a significant increase of tau expression in *Prnp0/0* could be observed. For comparison between groups we used the *student's t-test* (n = 5 per group in three independent experiments). Error bars indicate standard errors of the mean (SEM).

AβPP under physiological conditions without amyloid pathology.

PrP^C may inhibit the cleavage of AβPP via interaction with BACE1 and AβPP

The amyloid cascade hypothesis [42] implies that Aβ generation and deposition are the central events in the progression of AD. Aβ is formed during the amyloidogenic pathway of AβPP processing by cleavage of AβPP via β-secretase and γ-secretase. Recent studies on AD models indicated a causal involvement of PrP^C in the amyloid pathogenesis of AD [40, 41].

One of the caveats of the AβPP$_{mut}$ model are reports demonstrating that murine PrP^C has a different effect on the processing of AβPP$_{WT}$ and AβPP$_{mut}$ [43] and fails to reduce levels of Aβ and Aβ deposits in transgenic AβPP$_{Swe}$ PS1$_{L166P}$ mice [24]. Thus, we decided to use an alternative non-amyloid model to study the potential function of PrP^C.

Under our experimental conditions, both the α- and β-secretase pathways were inhibited by PrP^C indicating an unspecific inhibition of the AβPP cleavage.

However, the observed reduction after PrP^C upregulation in Aβ levels were more evident (up to 90%) in models using mutated AβPP$_{695}$ expressing cells [40] as compared to a physiological AβPP model, employed in this study, where the observed reduction in the levels of intra- and extracellular Aβ$_{40}$, sAβPPα, and sAβPPβ was approximately 25–30%. A reason might be that non-transfected HEK293 cells express a physiological level of AβPP. We conclude that the impact of PrP^C on the physiological AβPP processing seems to be moderate. The detection of amyloid fragments in the cell media indicates that the intracellular concentration of AβPP cleavage fragments might be regulated via secretion.

In mice, we observed that PrP^C may influence the processing of AβPP as indicated by a reduction in the amount of the AβPP cleavage fragment Aβ$_{40}$ without changing the concentration of γ-secretase. Brains of WT mice, independent of their age, contained a significantly lower amount of Aβ$_{40}$ compared to *Prnp0/0* mice, which is in line with our *in vitro* data. Interestingly, PrP^C-overexpressing Tg35 mice showed a further decrease of Aβ$_{40}$ levels when compared to WT mice. Others who housed the *Prnp0/0* mouse line, *Edinburgh 1* [40], are comparable to our findings, showing that the regulation of Aβ is independent of the mouse strain.

Our observation that AβPP or BACE1 level remained unchanged by PrP^C, even though the amount of several cleavage products was increased, is in line with other groups [24, 40]. One explanation may be that AβPP metabolism is more complex, e.g., AβPP can be processed by different pathways. Not all were influenced by PrP^C.

Another possibility to influence AβPP processing is via protein interaction which was investigated more detailed. Our data indicate that PrP^C can potentially interact with both proteins. While the PrP^C interaction with a pro-domain of an immature Golgi-associated form of BACE1, which may restrain BACE1 in the trans-Golgi network, had already been described previously [43], we additionally found that PrP^C might influence AβPP processing by binding to AβPP/sAβPP or the amyloid domain within AβPP. Our immunoprecipitation analysis revealed that PrP^C interacts with a secreted isoform of AβPP (sAβPP) as well as with full-length AβPP. However, the PrP^C-AβPP was faint in comparison to the PrP^C-sAβPP interaction. Conformational changes within full-length AβPP, which may at least partly bury the binding epitope of PrP^C, might serve as an explanation. Other studies which documented that PrP^C interacts with Aβ [22] or with an AβPP-like protein (Aplp1), which contains sequence similarities to AβPP [44], are in line with our findings.

Our data suggest that the binding of PrP^C to AβPP and the amyloid domain within AβPP may restrict the access for the processing secretase and impede the generation of amyloid fragments. In addition, an inhibition of BACE1 activity via PrP^C has already been reported [40, 45]. Furthermore, PrP^C is described as a physiological substrate of α-secretase. Its cleavage yields a number of PrP^C fragments [46] and can occur in competition with AβPP, showing that there might be different ways in which PrP^C may influence the processing of AβPP.

Remarkably, Vincent et al. detected a negative-feedback mechanism by which presenilins, the catalytic subunit of the γ-secretase complex, may control the transcription of PrP^C [47]. An increase of the amyloid intracellular domain (AICD), generated during the processing of AβPP by γ-secretase, can induce a p53-dependent upregulation of PrP^C mRNA level [47, 48].

Enhanced PrP^C levels may reduce the AD-like tau pathology

By regulating microtubule assembly and stabilization, tau can modulate cell motility and the efficacy of motor-driven transport processes [49]. AD and CJD

share several neuropathological characteristics. In particular, hyperphosphorylated tau deposits have been observed in a population of patients with Gerstmann-Straussler-Scheinker syndrome (GSS) bearing a certain point mutation on *PRNP* [50]. Immunohistochemical analysis had demonstrated a co-localization of p-tau and PrP in GSS [51], and it had also been shown that some mutated forms of PrP can form a complex with tau [52, 53]. These findings raise the question as to whether PrP^C might be involved in the regulation of tau protein and if the PrP^C-tau interaction may change the pathological characteristics of tau.

In our study, we identified two p-tau isoforms, Thr-181 and Ser-396, as potential interacting partners of PrP^C. An increased phosphorylation of tau at Thr-181 was shown to be an early event in the development of AD [54] and Ser-396 phosphorylation of tau is primarily responsible for the functional loss of tau-mediated tubulin polymerization [55].

Moreover, we confirmed the interaction of PrP^C and tau [30] in which the octa-repeat region of PrP^C and the N-terminus (1–91) or the tandem repeats region (amino acids 186–283) of tau are most probably involved [52].

A previous study even provided evidence that PrP^C may be involved in Aβ-induced hyperphosphorylation of tau [53], which strongly provides hints for an important role of PrP^C in AD.

To explore the role of PrP^C in tau pathology, we used a PrP^C overexpressing HEK293 cell model co-transfected with a 3PO-tau plasmid. The 3PO-tau model had been previously established for the investigation of the molecular mechanisms of tau pathology [31]. It is based on point mutations of intermitting breaking sequences of the microtubule-binding repeats of tau producing a rapid aggregation and cytotoxicity with accompanying occurrence of pathologic tau [31].

Interestingly, we found that the amount of 3PO-tau and p-tau (Ser-202 and Thr-205, both are AD-associated abnormal phosphorylation sites) was markedly reduced in different subcellular compartments when PrP^C is overexpressed, in particular within the cytoskeleton. Toxic effects of 3PO-tau were correlating with these findings, because a down regulation of 3PO-tau and p-tau in PrP^C overexpressing cells resulted in an increased cell survival compared to controls exhibiting an endogenous PrP^C level. Since the level of WT-tau was also modulated by PrP^C level, our data indicate an inhibitory and protective function of PrP^C under cellular stress condition induced by an increased level of tau.

To test this hypothesis, we examined the expression of tau and different forms of p-tau (Thr-181, Thr-231, Ser-199, and Ser-396) in a transgenic mice model lacking PrP^C. The regulation of tau phosphorylation is of utmost relevance for mediation of dynamic instabilities of microtubules. However, the expression of different p-tau isoforms, caused by different kinase activities, may differ in brains of scrapie infected hamsters [56], which was the reason why we analyzed different p-tau isoforms.

In our study we found that during the aging process, tau and p-tau levels were not abnormally changed in the brains of *Prnp0/0* mice compared to WT mice. Interestingly, under ischemic stress conditions, we observed a significant increase of tau in *Prnp0/0* mice which fits to our *in vitro* data.

The fact that PrP^C confers cell protection under cellular stress conditions is meanwhile widely accepted [14, 57, 58]. Under normal conditions, however, PrP^C seems to be less functional [33].

In this context, it remains elusive if PrP^C can suppress the production of tau, increase its proteolytical clearance, or even attenuate the aggregation of tau in AD. The observed reduction in a higher molecular weight form of 3PO-tau upon expression of PrP^C seems to suggest that this might be the case. A previous study showed a protective effect of PrP^C in huntingtin pathology. The outcome of this study that overexpression of PrP^C reduces huntingtin aggregation and toxicity in neuronal cells [59] fits our observations. The fact that a depletion of PrP^C causes a reduction in antioxidant enzymes and proteasome activity [59, 60] indicates that PrP^C might regulate the degradation process of 3PO-tau or p-tau. However, the exact molecular mechanism responsible for attenuation of 3PO-tau in PrP^C overexpression cells remains to be elucidated.

In conclusion, our data provide evidence for a protective function of PrP^C in AD. On the one hand, PrP^C may reduce the amount of potential harmful AβPP cleavage fragments and, on the other, it attenuates the production of tau *in vitro*. However, whether these findings can be assigned to an *in vivo* AD mice model or to AD patients requires further investigation.

ACKNOWLEDGMENTS

SUPPLEMENTARY MATERIAL

Supplementary figures and tables are available in the electronic version of this article: http://dx.doi.org/10.3233/JAD-130566.

REFERENCES

[1] Tobler I, Gaus SE, Deboer T, Achermann P, Fischer M, Rulicke T, Moser M, Oesch B, McBride PA, Manson JC (1996) Altered circadian activity rhythms and sleep in mice devoid of prion protein. *Nature* **380**, 639-642.

[2] Brown DR, Qin K, Herms JW, Madlung A, Manson J, Strome R, Fraser PE, Kruck T, von Bohlen A, Schulz-Schaeffer W, Giese A, Westaway D, Kretzschmar H (1997) The cellular prion protein binds copper *in vivo*. *Nature* **390**, 684-687.

[3] Brown DR, Schmidt B, Kretzschmar HA (1997) Effects of oxidative stress on prion protein expression in PC12 cells. *Int J Dev Neurosci* **15**, 961-972.

[4] Peters PJ, Mironov A Jr, Peretz D, van Donselaar E, Leclerc E, Erpel S, DeArmond SJ, Burton DR, Williamson RA, Vey M, Prusiner SB (2003) Trafficking of prion proteins through a caveolae-mediated endosomal pathway. *J Cell Biol* **162**, 703-717.

[5] Toni M, Spisni E, Griffoni C, Santi S, Riccio M, Lenaz P, Tomasi V (2006) Cellular prion protein and caveolin-1 interaction in neuronal cell line precedes Fyn/Erk1/2 signal transduction. *J Biomed Biotechnol* **69469**, 1-13.

[6] Schmitz M, Klöppner S, Klopfleisch S, Möbius W, Schwartz P, Zerr I, Althaus HH (2010) Mutual effects of caveolin and nerve growth factor signaling in pig oligodendrocytes. *J Neurosci Res* **88**, 572-588.

[7] Schmitz M, Zerr I, Althaus HH (2011) Effect of cavtratin, a caveolin-1 scaffolding domain peptide, on oligodendroglial signaling cascades. *Cell Mol Neurobiol* **31**, 991-997.

[8] Weiss E, Ramljak S, Asif AR, Ciesielczyk B, Schmitz M, Gawinecka J, Schulz-Schaeffer W, Behrens C, Zerr I (2010) Cellular prion protein overexpression disturbs cellular homeostasis in SH-SY5Y neuroblastoma cells but does not alter p53 expression: A proteomic study. *Neuroscience* **169**, 1640-1650.

[9] Nieznanski K, Nieznanska H, Skowronek KJ, Osiecka KM, Stepkowski D (2005) Direct interaction between prion protein and tubulin. *Biochem Biophys Res Commun* **334**, 403-411.

[10] Osiecka KM, Nieznanska H, Skowronek KJ, Karolczak J, Schneider G, Nieznanski K (2009) Prion protein region 23-32 interacts with tubulin and inhibits microtubule assembly. *Proteins* **77**, 279-296.

[11] Hachiya NS, Watanabe K, Sakasegawa Y, Kaneko K (2004) Microtubules-associated intracellular localization of the NH2-terminal cellular prion protein fragment. *Biochem Biophys Res Commun* **313**, 818-823.

[12] Nieznanski K, Podlubnaya ZA, Nieznanska H (2006) Prion protein inhibits microtubule assembly by inducing tubulin oligomerization. *Biochem Biophys Res Commun* **349**, 391-399.

[13] Martins VR, Brentani RR (2002) The biology of the cellular prion protein. *Neurochem Int* **41**, 353-355.

[14] Weise J, Crome O, Sandau R, Schulz-Schaeffer W, Bähr M, Zerr I (2004) Upregulation of cellular prion protein (PrP^C) after focal cerebral ischemia and influence of lesion severity. *Neurosci Lett* **372**, 146-150.

[15] Weise J, Sandau R, Schwarting S, Crome O, Wrede A, Schulz-Schaeffer W, Zerr I, Bähr M (2006) Deletion of cellular prion protein results in reduced Akt activation, enhanced postischemic caspase-3 activiation, and exacerbation of ischemic brain injury. *Stroke* **37**, 1296-1300.

[16] Schwarze-Eicke K, Keyvani K, Görtz N, Westaway D, Sachser N, Paulus W (2005) Prion protein (PrP^C) promotes beta-amyloid plaque formation. *Neurobiol Aging* **26**, 1177-1182.

[17] Takahashi RH, Tobiume M, Sato Y, Sata T, Gouras GK, Takahashi H (2011) Accumulation of cellular prion protein within dystrophic neurites of amyloid plaques in the Alzheimer's disease brain. *Neuropathology* **31**, 208-214.

[18] Del Bo R, Scarlato M, Ghezzi S, Martinelli-Boneschi F, Fenoglio C, Galimberti G, Galbiati S, Virgilio R, Galimberti D, Ferrarese C, Scarpini E, Bresolin N, Comi GP (2006) Is M129V of *PRNP* gene associated with Alzheimer's disease? A case-control study and a meta-analysis. *Neurobiol Aging* **27**, 770e1-770e5.

[19] Dermaut B, Croes EA, Rademakers R, Van den Broeck M, Cruts M, Hofman A, van Duijn CM, Van Broeckhoven C (2003) PRNP Val129 homozygosity increases risk for early-onset Alzheimer's disease. *Ann Neurol* **53**, 409-412.

[20] Riemenschneider M, Klopp N, Xiang W, Wagenpfeil S, Vollmert C, Müller U, Förstl H, Illig T, Kretschmar H, Kurz A (2004) Prion protein codon 129 polymorphism and risk of Alzheimer disease. *Neurology* **63**, 364-366.

[21] Berr C, Helbecque N, Sazdovitch V, Mohr M, Amant C, Amouyel P, Alpérovitch A, Hauw JJ (2003) Polymorphism of the codon 129 of the prion protein (PrP) gene and neuropathology of cerebral ageing. *Acta Neuropathol* **106**, 71-74.

[22] Laurén J, Gimbel DA, Nygaard HB, Gilbert JW, Strittmatter SM (2009) Cellular prion protein mediates impairment of synaptic plasticity by amyloid-beta oligomers. *Nature* **457**, 1128-1132.

[23] Nygaard HB, Strittmatter SM (2009) Cellular prion protein mediates the toxicity of beta-amyloid oligomers: Implications for Alzheimer disease. *Arch Neurol* **66**, 1325-1328.

[24] Gimbel DA, Nygaard HB, Coffey EE, Gunther EC, Laurén J, Gimbel ZA, Strittmatter SM (2010) Memory impairment in transgenic Alzheimer mice requires cellular prion protein. *J Neurosci* **30**, 6367-6374.

[25] Chung E, Ji Y, Sun Y, Kascsak RJ, Kascsak RB, Mehta PD, Strittmatter SM, Wisniewski T (2010) Anti-PrP^C monoclonal antibody infusion as a novel treatment for cognitive deficits in an Alzheimer's disease model mouse. *BMC Neurosci* **11**, 130.

[26] Caetano FA, Beraldo FH, Hajj GN, Guimaraes AL, Jürgensen S, Wasilewska-Sampaio AP, Hirata PH, Souza I, Machado CF, Wong DY, De Felice FG, Ferreira ST, Prado VF, Rylett RJ, Martins VR, Prado MA (2011) Amyloid-beta oligomers

increase the localization of prion protein at the cell surface. *J Neurochem* **117**, 538-553.

[27] Balducci C, Beeg M, Stravalaci M, Bastone A, Sclip A, Biasini E, Tapella L, Colombo L, Manzoni C, Borsello T, Chiesa R, Gobbi M, Salmona M, Forloni G (2010) Synthetic amyloid-beta oligomers impair long-term memory independently of cellular prion protein. *Proc Natl Acad Sci U S A* **107**, 2295-2300.

[28] Calella AM, Farinelli M, Nuvolone M, Mirante O, Moos R, Falsig J, Mansuy IM, Aguzzi A (2010) Prion protein and Abeta-related synaptic toxicity impairment. *EMBO Mol Med* **2**, 306-314.

[29] Kessels HW, Nguyen LN, Nabavi S, Malinow R (2010) The prion protein as a receptor for amyloid-beta. *Nature* **466**, E3-E4.

[30] Han J, Zhang J, Yao H, Wang X, Li F, Chen L, Gao C, Gao J, Nie K, Zhou W, Dong X (2006) Study on interaction between microtubule associated protein tau and prion protein. *Sci China C Life Sci* **49**, 473-479.

[31] Iliev AI, Ganesan S, Bunt G, Wouters FS (2006) Removal of pattern-breaking sequences in microtubule binding repeats produces instantaneous tau aggregation and toxicity. *J Biol Chem* **48**, 37195-37204.

[32] Shaw G, Morse S, Ararat M, Graham FL (2002) Preferential transformation of human neuronal cells by human adenoviruses and the origin of HEK 293 cells. *FASEB J* **16**, 869-871.

[33] Bueler H, Fischer M, Lang Y, Bluethmann H, Lipp HP, DeArmond SJ, Prusnier SB, Aguet M, Weissmann C (1992) Normal development and behavior of mice lacking the neuronal cell-surface PrP protein. *Nature* **356**, 577-582.

[34] Weidemann A, König G, Bunke D, Fischer P, Salbaum JM, Masters CL, Beyreuther K (1989) Identification, biogenesis, and localization of precursors of Alzheimer's disease A4 amyloid protein. *Cell* **57**, 115-126.

[35] Hilbich C, Mönning U, Grund C, Masters CL, Beyreuther K (1993) Amyloid-like properties of peptides flanking the epitope of amyloid precursor protein specific monoclonal antibody 22C11. *J Biol Chem* **268**, 26571-26577.

[36] Daebel V, Chinnathambi S, Biernat J, Schwalbe M, Habenstein B, Loquet A, Akoury E, Tepper K, Müller H, Baldus M, Griesinger C, Zweckstetter M, Mandelkow E, Vijayan V, Lange A (2012) β-Sheet core of tau paired helical filaments revealed by solid-state NMR. *J Am Chem Soc* **134**, 13982-13989.

[37] Dassie E, Andrews MR, Bensadoun JC, Cacquevel M, Schneider BL, Aebischer P, Wouters FS, Richardson JC, Hussain I, Howlett DR, Spillantini MG, Fawcett JW (2013) Focal expression of adeno-associated viral-mutant tau induces widespread impairment in an APP mouse model. *Neurobiol Aging* **34**, 1355-1368.

[38] Caillierez R, Bégard S, Lécolle K, Deramecourt V, Zommer N, Dujardin S, Loyens A, Dufour N, Aurégan G, Winderickx J, Hantraye P, Déglon N, Buée L, Colin M (2013) Lentiviral delivery of the human wild-type tau protein mediates a slow and progressive neurodegenerative tau pathology in the rat brain. *Mol Ther* **21**, 1358-1368.

[39] Yoshida H, Terada S, Ishizu H, Ikeda K, Hayabara T, Ikeda K, Deguchi K, Touge T, Kitamoto T, Kuroda S (2010) An autopsy case of Creutzfeldt-Jakob disease with a V180I mutation of the PrP gene and Alzheimer-type pathology. *Neuropathology* **30**, 159-164.

[40] Parkin ET, Watt NT, Hussain I, Eckman EA, Eckman CB, Manson JC, Baybutt HN, Turner AJ, Hooper NM (2007) Cellular prion protein regulates β-secretase cleavage of the

Alzheimer's amyloid precursor protein. *Proc Natl Acad Sci U S A* **104**, 11062-11067.

[41] Cisse M, Mucke L (2009) Alzheimer's disease: A prion protein connection. *Nature* **457**, 1090-1091.

[42] Hardy J, Allsop D (1991) Amyloid deposition as the central event in the aetiology of Alzheimer's disease. *Trends Pharmacol Sci* **12**, 383-388.

[43] Griffiths HH, Whitehouse IJ, Baybutt H, Brown D, Kellett KA, Jackson CD, Turner AJ, Piccardo P, Manson JC, Hooper NM (2011) Prion protein interacts with BACE1 protein and differentially regulates its activity toward wild type and Swedish mutant amyloid precursor protein. *J Biol Chem* **286**, 33489-33500.

[44] Yehiely F, Bamborough P, Da Costa M, Perry BJ, Thinakaran G, Cohen FE, Carlson GA, Prusiner SB (1997) Identification of candidate proteins binding to prion protein. *Neurobiol Dis* **3**, 339-355.

[45] Hooper NM, Turner AJ (2008) A new take on prions: Preventing Alzheimer's disease. *Trends Biochem Sci* **33**, 151-155.

[46] Cisse MA, Sunyach C, Lefranc-Jullien S, Postina R, Vincent B, Chacler F (2005) The disintegrin ADAM9 indirectly contributes to the physiological processing of cellular prion by modulating ADAM 10 activity. *J Biol Chem* **280**, 40624-40631.

[47] Vincent B, Sunyach C, Orzechowski HD, St George-Hyslop P, Checler F (2009) p53-dependent transcriptional control of cellular prion by presenilins. *J Neurosci* **29**, 6752-6760.

[48] Kellett KA, Hooper NM (2009) Prion protein and Alzheimer disease. *Prion* **3**, 190-194.

[49] Lee VMY, Giasson BI, Trojanowski JQ (2004) More than just two peas in a pod: Common amyloidogenic properties of tau and alphasynuclein in neurodegenerative diseases. *Trends Neurosci* **27**, 129-134.

[50] Ghetti B, Tagliavini F, Giaccone G, Bugiani O, Frangione B, Farlow MR, Dlouhy SR (1994) Familial Gerstmann-Sträussler-Scheinker disease with neurofibrillary tangles. *Mol Neurobiol* **8**, 41-48.

[51] Ishizawa K, Komori T, Shimazu T, Yamamoto T, Kitamoto T, Shimazu K, Hirose T (2002) Hyperphosphorylated tau deposition parallels prion protein burden in a case of Gerstmann-Sträussler-Scheinker syndrome P102L mutation complicated with dementia. *Acta Neuropathol* **104**, 342-350.

[52] Wang XF, Dong CF, Zhang J, Wan YZ, Li F, Huang YX, Han L, Shan B, Gao C, Han J, Dong XP (2008) Human tau protein forms complex with PrP and some GSS- and fCJD-related PrP mutants possess stronger binding activities with tau *in vitro*. *Mol Cell Biochem* **310**, 49-55.

[53] Larson M, Sherman MA, Amar F, Nuvolone M, Schneider JA, Bennett DA, Aguzzi A, Lesné SE (2012) The complex PrP(c)-Fyn couples human oligomeric Aβ with pathological tau changes in Alzheimer's disease. *J Neurosci* **32**, 16857-16871.

[54] Hansson O, Zetterberg H, Buchhave P, Londos E, Blennow K, Minthon L (2006) Association between CSF biomarkers and incipient Alzheimer's disease in patients with mild cognitive impairment: A follow-up study. *Lancet Neurol* **5**, 228-234.

[55] Evans DB, Rank KB, Bhattacharya K, Thomsen DR, Gurney ME, Sharma SK (2000) Tau phosphorylation at serine 396 and serine 404 by human recombinant tau protein kinase II inhibits tau's ability to promote microtubule assembly. *J Biol Chem* **275**, 24977-24983.

[56] Wang GR, Shi S, Gao C, Zhang BY, Tian C, Dong CF, Zhou RM, Li XL, Chen C, Han J, Dong XP (2010) Changes of tau profiles in brains of the hamster infected with scrapie strains

263 K or 139 A possibly associated with the alteration of phosphate kinases. *BMC Infect Dis* **10**, 86.

[57]   Walz R, Amaral OB, Rockenbach IC, Roesler R, Izquierdo I, Cavalheiro EA, Martins VR, Brentani RR (1999) Increased sensitivity to seizures in mice lacking cellular prion protein. *Epilepsia* **40**, 1679-1682.

[58]   McLennan NF, Brennan PM, McNeill A, Davies I, Fotheringham A, Rennison KA, Ritchie D, Brannan F, Head MW, Ironside JW, Williams A, Bell JE (2004) Prion protein accumulation and neuroprotection in hypoxic brain damage. *Am J Pathol* **165**, 227-235.

[59]   Lee KJ, Panzera A, Rogawski D, Greene LE, Eisenberg E (2007) Cellular prion protein (PrP^C) protects neuronal cells from the effect of huntingtin aggregation. *J Cell Sci* **120**, 2663-2671.

[60]   Klamt F, Dal-Pizzol F, Conte da Frota ML Jr, Walz R, Andrades ME, da Silva EG, Brentani RR, Izquierdo I, Fonseca Moreira JC (2001) Imbalance of antioxidant defense in mice lacking cellular prion protein. *Free Radic Biol Med* **30**, 1137-1144.